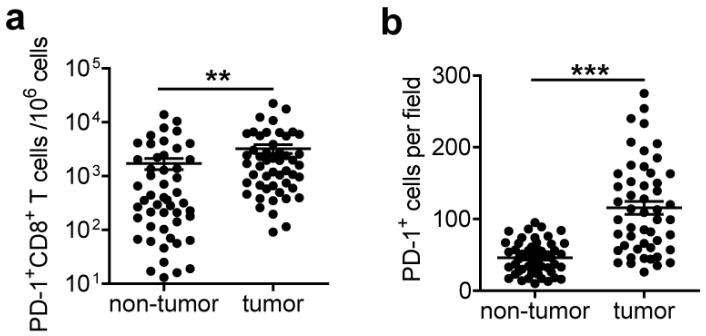

Supplemental Figure 1. PD-1$^+$ cell numbers in the non-tumor and tumor tissues of 50 GC patients. **a** The total number of PD-1$^+$CD8$^+$ T cells per million cells was calculated in the non-tumor and tumor tissues of GC patients based on gated PD-1$^+$CD8$^+$ cell percentages. **b** The number of PD-1$^+$ cells per field was statistically analyzed in the non-tumor and tumor tissues of GC patients based on immunohistochemical staining. ***P*<0.01, ****P*<0.001: Student's *t* test

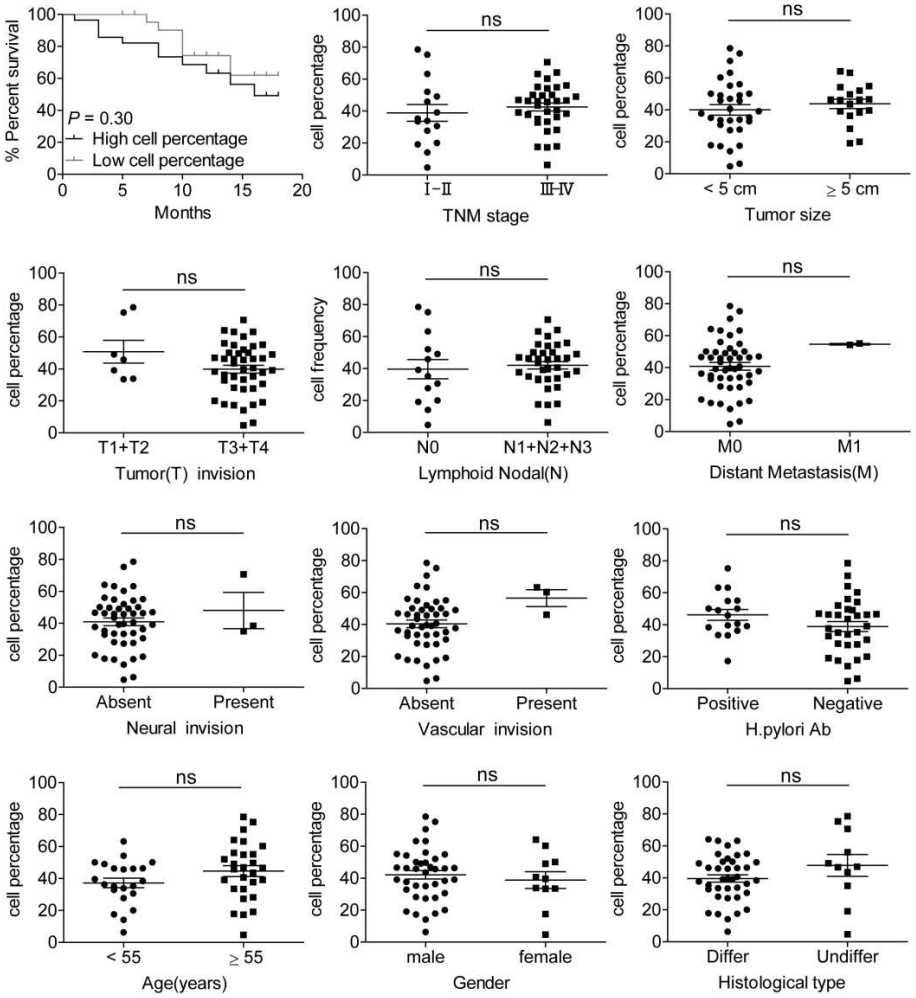

Supplemental Figure 2. Correlation analysis between the percentage of tumor-infiltrating PD-1$^+$CD8$^+$ T cells and various clinical parameters of GC patients. For the cumulative survival curves, patients were separated into two groups by the median value of tumor-infiltrating PD-1$^+$CD8$^+$ T cell percentages, and Kaplan–Meier plots were used to calculate cumulative survival differences. Each dot represents one patient. Ab, antibody; Diff, differentiated; Undiff, undifferentiated; ns, not significant.

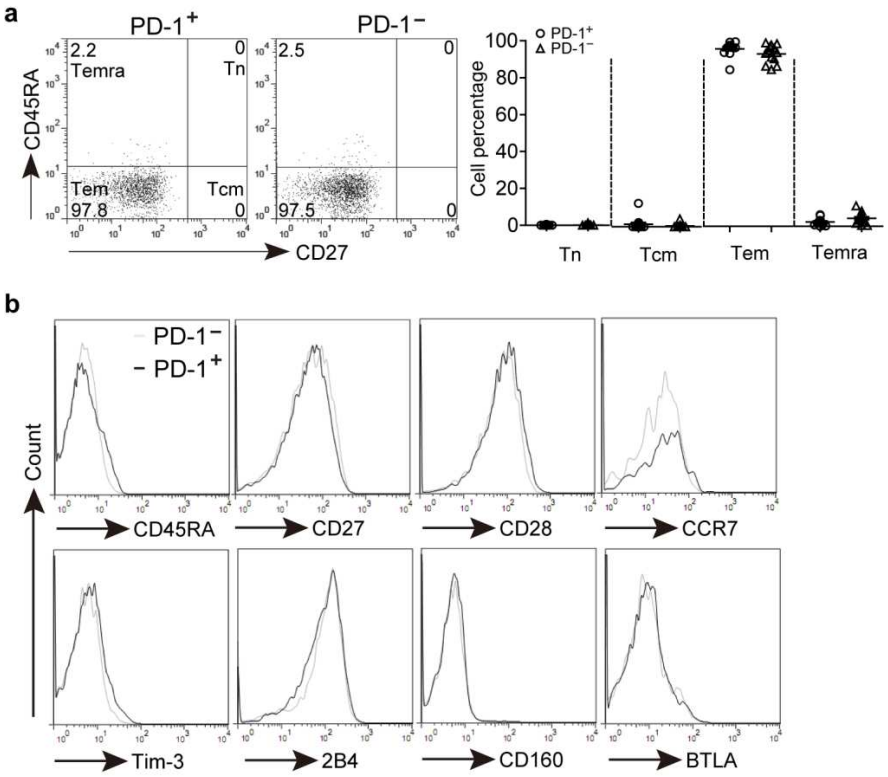

Supplemental Figure 3. Phenotypic features of GC-infiltrating PD-1$^+$CD8$^+$ T cells. **a** Tumor tissue-derived cell suspensions were stained with CD3, CD8, PD-1, CD45RA and CD27 antibodies. A representative flow cytometry analysis from one sample and the percentages of different PD-1$^+$CD8$^+$ versus PD-1$^-$CD8$^+$ T cell groups indicated by CD45RA and CD27 expression are shown: Tn (CD45RA$^+$CD27$^+$), Tcm (CD45RA$^-$CD27$^+$), Tem (CD45RA$^-$CD27$^-$), and Temra (CD45RA$^+$CD27$^-$). **b** Tumor-derived cell suspensions were stained with CD3, CD8, PD-1, CD45, CD27, CD28, CCR7, Tim-3, 2B4, CD160 and BTLA antibodies. Cells were gated on PD-1$^+$CD8$^+$ and PD-1$^-$CD8$^+$ T cells, and the expression of CD45, CD27, CD28, CCR7, Tim-3, 2B4, CD160 and BTLA was analyzed.

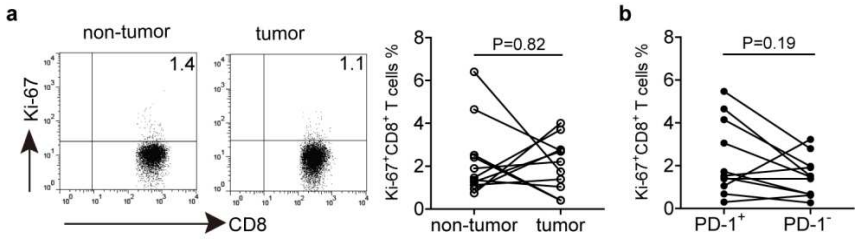

Supplemental Figure 4. The expression of proliferation-associated marker Ki-67 in PD-1$^+$CD8$^+$ T cells in GC. Tumor and non-tumor tissue-derived cell suspensions were stained with CD3, CD8 and PD-1 antibodies, and then cells were fixed and permeabilized for 30 min using Foxp3-Staining Buffer Set (eBiosciences), following stained with a Ki-67 antibody for flow cytometric analysis. **a** Representative dot-plots and statistical analysis showing the percentages of Ki-67 expression among CD8$^+$ T cells from paired tumor and non-tumor tissues of 11 GC patients. **b** Statistical analysis of Ki-67$^+$ cell percentages on PD-1$^+$CD8$^+$ versus PD-1$^-$CD8$^+$ T cells in the tumor tissues of 11 GC patients.

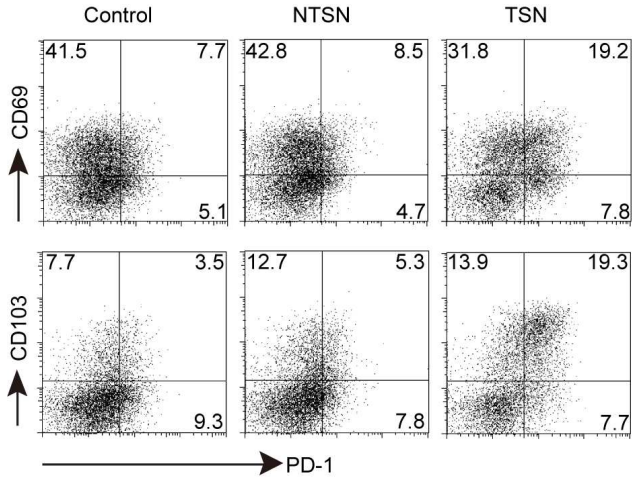

Supplemental Figure 5. GC-derived soluble factor(s) contribute to PD-1 expression of $CD8^+$ T cells. $CD8^+$ T cells were isolated and cultured with 30% TSN or NTSN for 72 hours, and then the levels of PD-1, CD69 and CD103 expression on these $CD8^+$ T cells were analyzed.

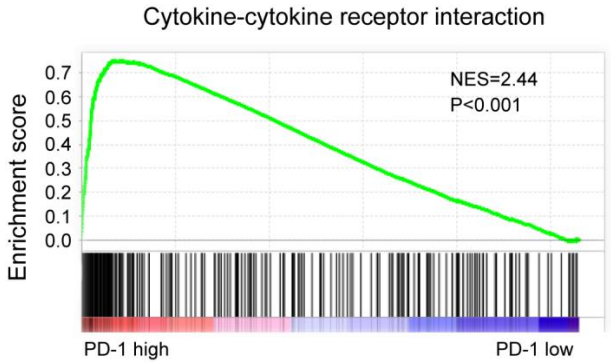

Supplemental Figure 6. Gene set enrichment analysis (GSEA) revealed an enrichment of cytokine-cytokine receptor interaction involved in PD-1^{high} tumors. NES, non-enrichment score. GSEA performed by the Molecular Signature Database (MSigDB) was used to identify the pathways that might be significantly enriched in PD-1^{high} tumor samples. If a gene set has a positive enrichment score and the majority of its members also have higher expression accompanied with higher risk score, the set is then termed 'enriched'.

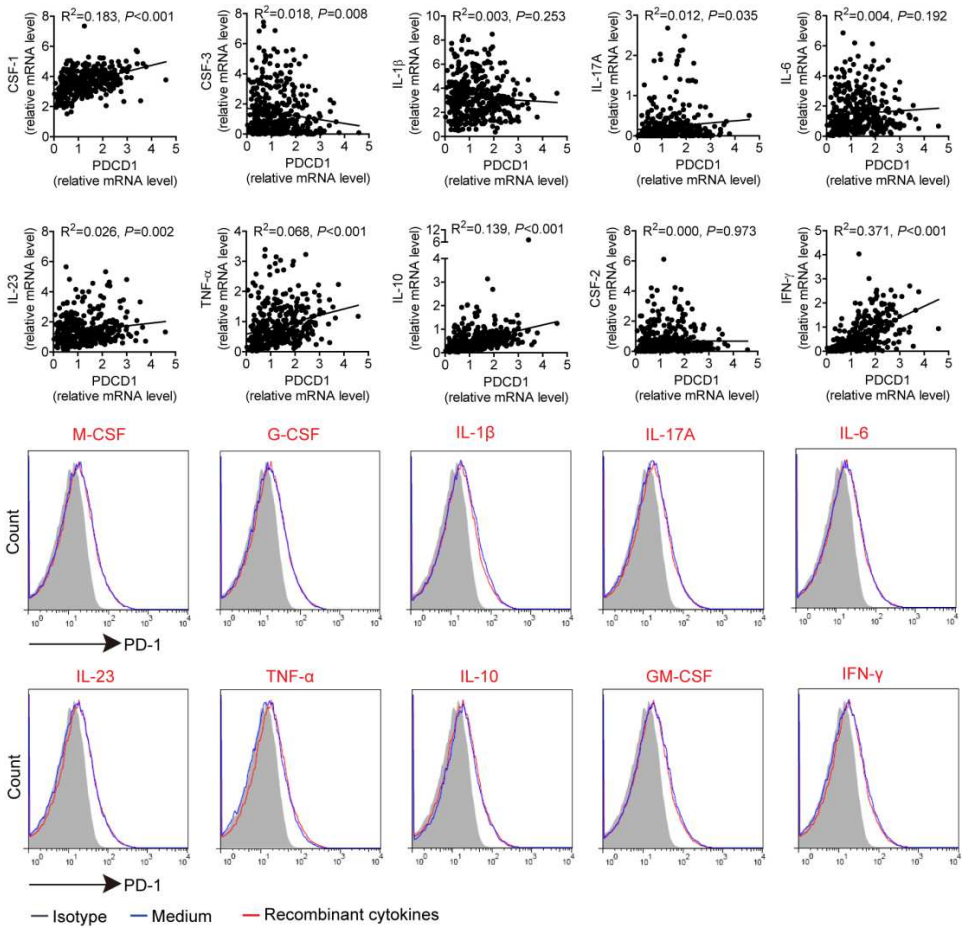

Supplemental Figure 7. The expression of PD-1 on $CD8^+$ T cells after stimulation. The dataset of gene expression profiles in GC patients were downloaded from the Cancer Genome Atlas (TCGA) data portal website (https://tcga-data.nci.nih.gov/tcga/). We obtained the normalized reads from 384 GC patients by summing up the raw counts, and then the correlation analysis between PD-1 transcript (PDCD1) level and CSF-1 (M-CSF transcript), CSF-3 (G-CSF transcript), IL-1β, IL-17A, IL-6, IL-23, TNF-α, IL-10, CSF-2 (GM-CSF transcript), and IFN-γ mRNA level were performed in 384 GC patients from TCGA dataset. Blood $CD8^+$ T cells were purified and cultured for 72 hours with 10 ng/ml of individual recombinant human M-CSF, G-CSF, IL-1β, IL-17A, IL-6, IL-23, TNF-α, IL-10, GM-CSF, and IFN-γ in the presence of anti-CD3 and anti-CD28 antibodies. A representative histogram of PD-1 expression on $CD8^+$ T cells by flow cytometry.

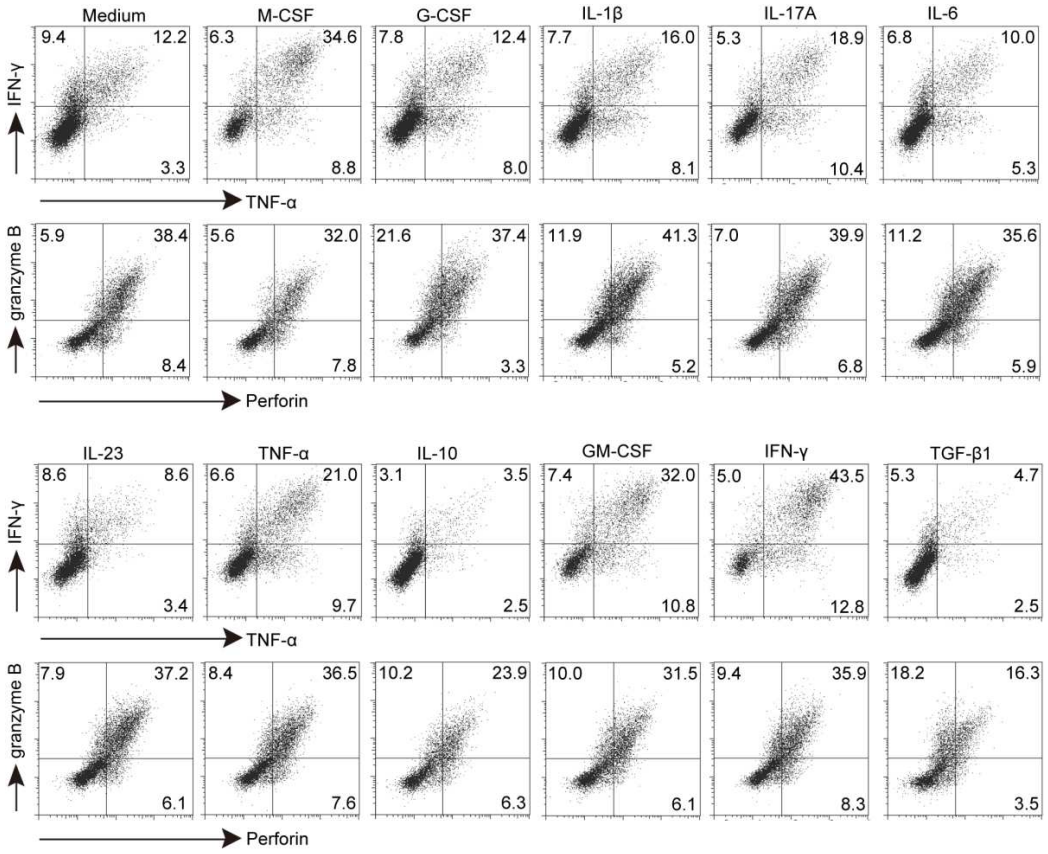

Supplemental Figure 8. The effector function of $CD8^+$ T cells after stimulation. Blood $CD8^+$ T cells were purified and cultured for 72 hours with 10 ng/ml of individual recombinant human M-CSF, G-CSF, IL-1β, IL-17A, IL-6, IL-23, TNF-α, IL-10, GM-CSF, IFN-γ and TGF-β1 in the presence of anti-CD3 and anti-CD28 antibodies. The expressions of INF-γ, TNF-α, granzyme B and perforin in these $CD8^+$ T cells were determined by flow cytometry.

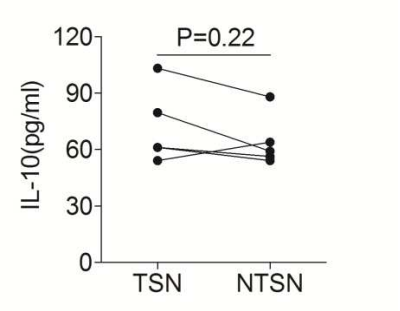

Supplemental Figure 9. The comparison of IL-10 levels between TSN and NTSN. TSN and NTSN obtained from 5 selected GC patients were detected by using IL-10 ELISA kits in accordance with the manufacturer's recommendations (Dakewei Biotech), and statistical analysis of the concentrations of IL-10 was performed between TSN and NTSN.

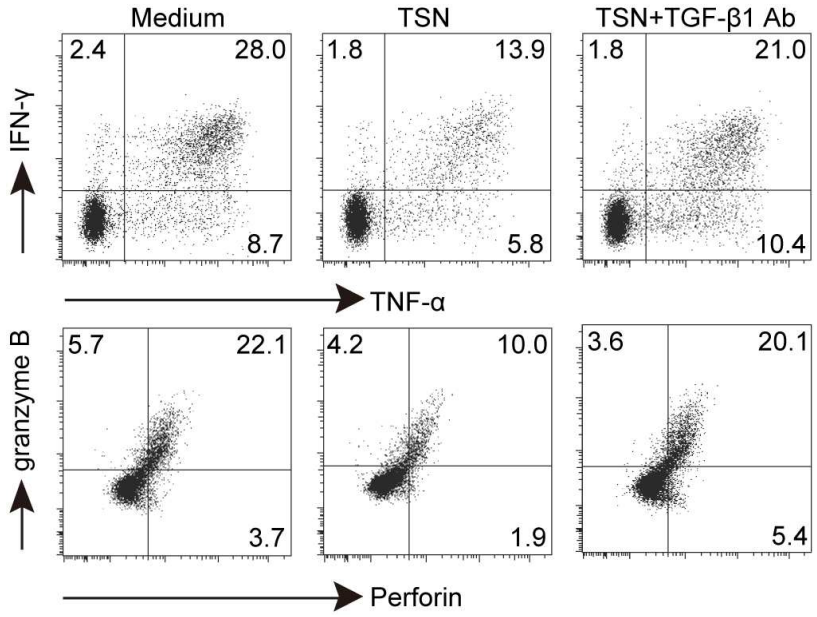

Supplemental Figure 10. TSN-induced $CD8^+$ T cell dysfunction was reversed by TGF-β1 blockade. TSN-treated $CD8^+$ T cells were cultured with or without a TGF-β1 blocking antibody for 72 hours in the presence of anti-CD3 and anti-CD28 antibodies. $CD8^+$ T cells producing INF-γ, TNF-α, granzyme B and perforin were determined by flow cytometry.

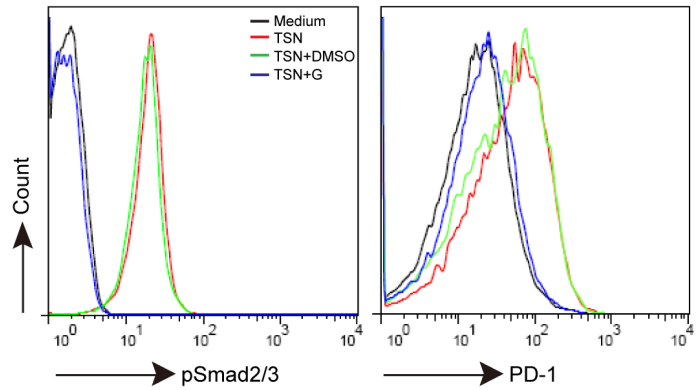

Supplemental Figure 11. TSN-induced Smad2/3 phosphorylation and PD-1 expression of $CD8^+$ T cells was blocked by a TGF-βRI inhibitor. $CD8^+$ T cells were pretreated with or without DMSO or Galunisertib (G, a TGF-βRI kinase inhibitor, 5 μM) for 1 hour, and then cultured with 30% TSN in the presence of anti-CD3 and anti-CD28 antibodies, and the level of Smad2/3 phosphorylation and PD-1 expression of $CD8^+$ T cells were determined by flow cytometry.

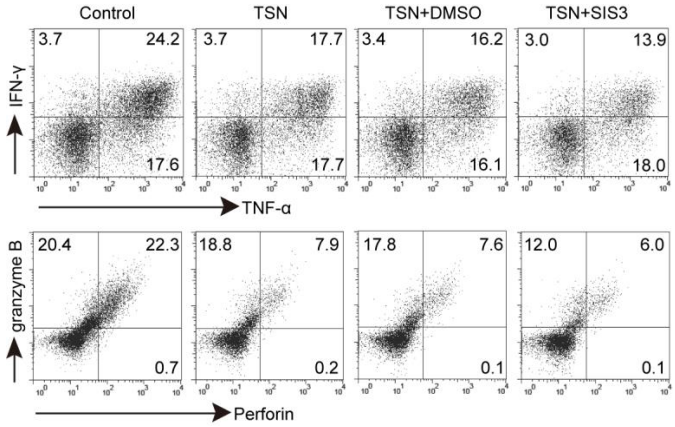

Supplemental Figure 12. GC-derived TGF-β1 mediated Smad3-independent $CD8^+$ T cell dysfunction. $CD8^+$ T cells were purified from PBMCs and pretreated with or without SIS3 or DMSO for 1 hour, and then exposed to 30% TSN for 72 hours in the presence of anti-CD3 and anti-CD28 antibodies. The expression of IFN-γ, TNF-α, granzyme B and perforin of $CD8^+$ T cells were analyzed by flow cytometry in the Control group, TSN-treated group, TSN plus DMSO group and TSN plus SIS3 group.

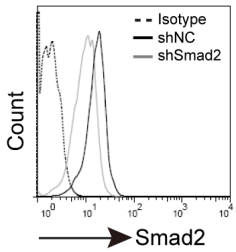

Supplemental Figure 13. The expression of Smad2 in $CD8^+$ T cells transduced with lentiviral particles. $CD8^+$ T cells purified from PBMCs were activated with pre-coated with anti-CD3 (2 μg/ml) and anti-CD28 (1 μg/ml) antibodies for 24 hours, and then lentiviral particles containing Smad2 shRNA (shSmad2, Santa Cruz Biotechnology) or control shRNA (shNC, Santa Cruz Biotechnology) were added. After 72 hours transduction, Cells were washed and fixed, permeabilized for 30 min using Foxp3-Staining Buffer Set (eBiosciences), following stained with Alexa Fluor® 488 conjugated anti-human Smad2 antibody (Santa Cruz Biotechnology) for flow cytometric analysis.

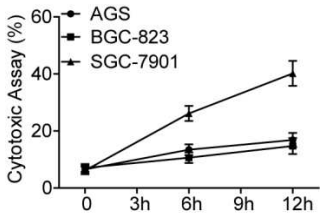

Supplemental Figure 14. The cytotoxicity effect of $CD8^+$ T cells on SGC-7901, AGS and BGC-823 cells. $CD8^+$ T cells activated *in vitro* were plated in 96-well plates with mitomycin C- (10 μg/ml, Sigma-Aldrich) treated gastric cancer cell lines SGC-7901, AGS or BGC-823 for different time (0, 6 and 12 hours), and the effector/target cell (E: T) ratio used was 10:1. Cytotoxicity was assayed by using the CytoTox 96® Non-Radioactive Cytotoxicity Assay (Promega) according to manufacturer's instructions. Cytotoxicity%= (Experimental-Effector Spontaneous-Target Spontaneous) / (Target Maximum-Target Spontaneous) × 100.

Supplemental Table 1. Clinical Characteristics of 50 GC Patients

Variables	No. of patients
Sex (male/female)	39/11
Age (*y*), median (range)	55, 28-82
H pylori antibody (positive/negative)	17/33
Tumor size (cm; <5/≥5)	32/18
Histologic type (differentiated/undifferentiated)	11/39
Neural invasion (absent/present)	47/3
Vascular invasion (absent/present)	47/3
Tumor (T) invasion (T1+T2/T3+T4)	7/43
Lymphoid nodal (N) status (N0 / N1+N2+N3)	14/36
Distant metastasis (M) status (M0/M1)	58/2
TNM stage (I+II/III+IV)	16/34
PD^+CD8^+ T cell percentage (median, range)	42.1, 4.7-78.5

Supplemental Table 2. Fluorochrome-conjugated antibodies used in flow cytometry

Antibodies	Source	Clone
Alexa Fluor 488 conjugated anti-human CD160	eBioscience	BY55
APC-H7 conjugated anti-human CD3	BD Pharmingen	SK7
APC-conjugated anti-human PD-1	Biolegend	EH12.2H7
FITC-conjugated anti-human CD45RA	Biolegend	HI100
FITC-conjugated anti-human CD69	Biolegend	FN50
FITC-conjugated anti-human CD62L	Biolegend	DREG-56
FITC-conjugated anti-human CD160	Biolegend	DX22
FITC-conjugated anti-human granzyme B	Biolegend	GB11
FITC-conjugated anti-human IFN-γ	Biolegend	B27
FITC-conjugated anti-human Eomes	eBioscience	WD1928
PE-conjugated anti-human Perforin	Biolegend	dG9
PE-conjugated anti-human CD103	Biolegend	Ber-ACT8
PE-conjugated anti-human CD25	Biolegend	BC96
PE-conjugated anti-human PD-1	Biolegend	EH12.2H7
PE-conjugated anti-human Tim-3	Biolegend	F38-2E2
PE-conjugated anti-human BTLA	Biolegend	MIH26
PE-conjugated anti-human 2B4	Biolegend	C1.7
PE-conjugated anti-human T-bet	Biolegend	eBio4B10 (4B10)
PE-conjugated anti-human TNF-α	Biolegend	MAb11
PE-Cy7-conjugated anti-human CD27	Biolegend	M-T271
PE-Cy7-conjugated anti-human CD45	Biolegend	HI30
PE-Cy7-conjugated anti-human CCR7	Biolegend	G043H7
PE-Cy7-conjugated anti-human CD28	Biolegend	CD28.2
PE-Cy7-conjugated anti-human IFN-γ	Biolegend	A019D5
PerCP-Cy5.5-conjugated anti-human CD8	Biolegend	RPA-T8